Eur. Phys. J. D **41**, 113–119 (2007)
DOI: 10.1140/epjd/e2006-00178-y

THE EUROPEAN PHYSICAL JOURNAL D

Melting, freezing and nucleation in nanoclusters of potassium chloride

II - Modelling the solid-liquid coexistence

P.C.R. Rodrigues and F.M.S. Silva Fernandes[a]

Department of Chemistry and Biochemistry, Faculty of Sciences, University of Lisboa, Campo Grande, Bloco C8, 1749-016 Lisboa, Portugal

Received 5 June 2006 / Received in final form 4 July 2006
Published online 5 August 2006 –

Abstract. In a recent article we have reported extensive molecular dynamics simulations for the melting freezing and nucleation in unconstrained nanoclusters of KCl. Based on that study we propose, in the present article, a theoretical model for the solid-liquid coexistence in finite systems, at virtually zero external pressure and no vaporisation. The main trends of the phase coexistence behaviour, namely the starting and the end points, are explained by the model as a function of system size. Other specific properties of clusters, eventually accessible by experiment, are defined and their values predicted. On the absence of available experimental data, the model is tested against simulation results with fairly good accordance.

PACS. 61.46.-w Nanoscale materials: clusters, nanoparticles, nanotubes, and nanocrystals – 64.70.Nd Structural transitions in nanoscale materials

1 Introduction

Several authors have discussed theoretical models for phase coexistence in clusters, namely in what concerns the melting point [1], the solid-liquid, solid-vapour [2,3] and vapour-liquid equilibria [4]. In these works equilibrium is established between a finite phase immersed in a bulk phase, corresponding to the limit conditions of the initial or final stages of a transition where the emerging/vanishing phases present deviations from bulk properties due to size effects on the free energy. Three well known cases [3] are: (a) formation of a liquid droplet inside the vapour contained in a vessel with volume V at temperature T, whose solution is Laplace's equation; (b) formation of the droplet at pressure p and temperature T, whose solution is Thomson-Gibbs's equation; and (c) formation of a crystal inside the liquid (or vapour) in a vessel of volume V at temperature T, that corresponds to Gibbs-Curie-Wulff's theorem. In the same context, Cleveland and collaborators [5] presented the "cluster wetting model", where the parametric determination of the free energy of a cluster as a function of the molar fractions of the phases (considered to be in a geometry of overlapping spheres) is used to compute the most favourable wetting conditions of a system at temperature T and zero pressure, depending on the interfacial energy densities of the material.

[a] e-mail: fsilva@fc.ul.pt

The present model aims at predicting the conditions of solid-liquid coexistence in unconstrained clusters, at virtually zero external pressure and no vaporisation, and correlating their properties. Similarly, for example, to the use of arbitrary geometries or the omission of surface curvature effects [5–8], some approximations shall also be considered to the general problem concerned with the various phase and inter-phase contributions.

Clusters behave differently from the corresponding bulk systems, mainly in phase change or phase coexistence regions. However, they asymptotically approach the bulk properties as the size increases. This is just the basis of the proposed model. It is assumed that a given cluster has a virtual bulk-like behaviour which is taken as the reference state. The model traces out the deviations relatively to the reference state, which are dependent on the number of particles, n. All the derived equations should then yield the right bulk limit when $n \to \infty$.

Section 2 presents the model and its limitations. The model application to phase diagrams of potassium chloride clusters is discussed in Section 3. Section 4 contains the derivation of other properties, eventually accessible by experiment, and their comparison with simulation results. Finally, Section 5 presents the concluding remarks.

2 The model

In a bulk system, after the melting onset and solid-liquid equilibrium is attained, adding energy to the system

converts a portion of solid to liquid, with the temperature and pressure remaining constant. The number of solid ions in the bulk system, n_s^∞, at a given energy E, is:

$$n_s^\infty = \frac{E_{\mathrm{l}(T_\mathrm{m})} - E}{E_{\mathrm{l}(T_\mathrm{m})} - E_{\mathrm{s}(T_\mathrm{m})}} n \tag{1}$$

where $E_{\mathrm{s}(T_\mathrm{m})}$ and $E_{\mathrm{l}(T_\mathrm{m})}$ are, respectively, the total energies of the bulk solid and liquid at the melting temperature T_m, and n is the total number of particles in the system.

However, a finite system (cluster) prepared at any fixed total energy over the bulk solid-liquid line shall always have a size less than the critical nucleus (see Eq. (5)) at T_m. Therefore, at those fixed energies a number of solid ions, Δn_s, shall be transferred to the liquid until the cluster reaches a temperature $T < T_\mathrm{m}$ at which the corresponding solid critical nucleus can sustain equilibrium with the liquid. If the conversion of solid ions into liquid was realized at constant temperature, it would require an external energy $[\Delta n_\mathrm{s}/n]\,\Delta h$, to compensate for the increase of potential energy. For the clusters, in the conditions mentioned above, that conversion is realized at constant total energy, so the increase of potential energy is entirely obtained at the cost of the internal kinetic energy. This results in a decrease of the cluster temperature, $\Delta T = T - T_\mathrm{m}$,

$$\Delta T = \frac{\Delta n_\mathrm{s} \Delta h}{n C_p} \tag{2}$$

where Δh is the enthalpy of melting and C_p is the heat capacity.

The number of solid ions in the cluster, at energy E, as a function of temperature is obtained from:

$$n_\mathrm{s} = n_s^\mathrm{bb} + \Delta n_\mathrm{s} \tag{3}$$

where n_s^bb, given by the same form of equation (1), should be understood as the number of solid ions that the cluster would have if it followed the bulk behaviour. $E_{\mathrm{s}(T_\mathrm{m})}$ and $E_{\mathrm{l}(T_\mathrm{m})}$ are, now, the solid and liquid cluster energies at the bulk melting temperature, T_m, which depend, of course, on the cluster size.

Substituting n_s^bb from (1) and Δn_s from (2):

$$n_\mathrm{s} = \frac{E_{\mathrm{l}(T_\mathrm{m})} - E}{\Delta h} n + \frac{(T - T_\mathrm{m}) n C_p}{\Delta h}. \tag{4}$$

In a first order approximation, we can take the bulk value for Δh [9]. However, Δh is also a function of the number of particles. This aspect shall be taken into account in a second order approximation presented in Section 2.1. Incidentally, it is noteworthy that equation (4) yields the right bulk limit when $n \to \infty$. Relatively to C_p, it seems plausible to take it, in a first approximation, as the average of the solid and liquid values at the start and end of melting, since that values do not differ much for alkali halide clusters [10]. However, for systems which have very distinct solid and liquid heat capacities a better approximation may be needed.

The size of the critical nucleus, n^*, at the melting temperature, T_m, approaches infinity according to the following equation, derived elsewhere [10,11]:

$$n^* = \left[\frac{4 \upsilon^{\frac{2}{3}} \sigma T_\mathrm{m}}{(T_\mathrm{m} - T) \Delta h} \right]^3 \tag{5}$$

where υ is the specific volume of the solid, σ is the surface tension in the interface, and Δh is the enthalpy of melting. Equation (5) was obtained, without loss of generality, for a cubic nucleus (inside a bulk liquid phase) in order to be in accordance with the symmetry of the available simulation data for KCl. Moreover, according to the results of our previous work [10], it is assumed that equation (5) is a fairly good approximation even when the liquid phase is not infinite and the nucleus is not completely wetted.

The size of the cubic critical nucleus can be recast in a more compact form:

$$n^* = k^3 \frac{{T_\mathrm{m}}^3}{(T_\mathrm{m} - T)^3} \tag{6}$$

where

$$k^3 = \left[\frac{4 \upsilon^{\frac{2}{3}} \sigma}{\Delta h} \right]^3. \tag{7}$$

Phase equilibrium is attained when the crystallite size, given by equation (4), becomes equal to the size of the critical nucleus, given by equation (6), that is, when the temperature T is a root of:

$$\frac{E_{\mathrm{l}(T_\mathrm{m})} - E}{\Delta h} n + \frac{(T - T_\mathrm{m}) n C_p}{\Delta h} - k^3 \frac{{T_\mathrm{m}}^3}{(T_\mathrm{m} - T)^3} = 0. \tag{8}$$

From equation (8):

$$E = E_{\mathrm{l}(T_\mathrm{m})} + (T - T_\mathrm{m}) C_p - k^3 \frac{\Delta h\, {T_\mathrm{m}}^3}{n (T_\mathrm{m} - T)^3}. \tag{9}$$

This is the key equation to work out the predicted (T, E) values for direct comparison with the results from simulations.

Figure 1 represents the crystallite (n_s) and critical nucleus (n^*) sizes, at different energies, as a function of temperature, given by equations (4) and (6) respectively.

The lower temperature where coexistence still exists can be obtained noting that (4) and (6) are tangent at that point (see Fig. 1)

$$T_\mathrm{inf} = T_\mathrm{m} - \left(\frac{3 k^3\, {T_\mathrm{m}}^3\, \Delta h}{n C_p} \right)^{\frac{1}{4}} \tag{10}$$

and the correspondent energy is

$$E(T_\mathrm{inf}) = E_{\mathrm{l}(T_\mathrm{m})} + \frac{\Delta h}{n} \left[\frac{(T_\mathrm{inf} - T_\mathrm{m}) n C_p}{\Delta h} - k^3 \frac{{T_\mathrm{m}}^3}{(T_\mathrm{m} - T_\mathrm{inf})^3} \right]. \tag{11}$$

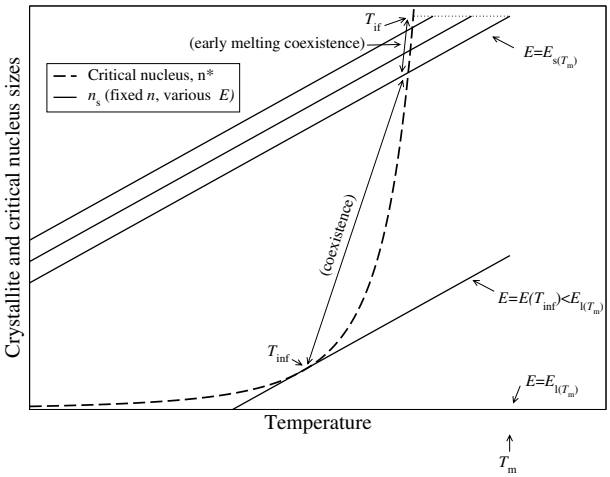

Fig. 1. Graphical construction, built from equations (4) and (6), to determine the limits of the phase coexistence for an arbitrary cluster.

The lowest energy where coexistence, predicted by equation (8), is possible can be obtained noting that the temperature along the solid curve, near the melting point, is

$$T_{\mathrm{s}} = T_{\mathrm{m}} - \frac{E_{\mathrm{s}(T_{\mathrm{m}})} - E}{C_p} \tag{12}$$

and equating it to temperature T in equation (6) with $n^* = n$:

$$E_{\mathrm{if}} = E_{\mathrm{s}(T_{\mathrm{m}})} - kC_p T_{\mathrm{m}} n^{-\frac{1}{3}}. \tag{13}$$

Melting in the energy interval $\left]E_{\mathrm{if}}, E_{\mathrm{s}(T_{\mathrm{m}})}\right[$ shall be, from now on, designated as early melting, for the bulk-like conditions have been chosen for clusters. However, this does not mean an exceptional situation. Indeed, at the present approximation level, the model always predicts the cluster melting onset at lower temperatures and energies than the ones of the corresponding bulk systems.

The temperature correspondent to the energy E_{if} is (see Fig. 1)

$$T_{\mathrm{if}} = T_{\mathrm{m}}\left(1 - kn^{-\frac{1}{3}}\right). \tag{14}$$

The domain of T values for the resolution of the equation model in order to E is bounded by T_{if} and T_{inf}.

2.1 Second order approximation to Δh

The dependence of Δh on the number of particles can be found considering:

$$E_{\mathrm{l}(T_{\mathrm{m}})} = E^{\infty}_{\mathrm{l}(T_{\mathrm{m}})} + \varsigma_{\mathrm{l}} n^{-\frac{1}{3}} \tag{15}$$

$$E_{\mathrm{s}(T_{\mathrm{m}})} = E^{\infty}_{\mathrm{s}(T_{\mathrm{m}})} + \varsigma_{\mathrm{s}} n^{-\frac{1}{3}} \tag{16}$$

hence

$$\Delta h = \Delta h^{\infty} + \Delta\varsigma n^{-\frac{1}{3}}. \tag{17}$$

The value of k is also dependent on n:

$$k = \frac{4\upsilon^{\frac{2}{3}}\sigma}{\Delta h^{\infty} + \Delta\varsigma n^{-\frac{1}{3}}}. \tag{18}$$

The limit value $k^{\infty} = 4\upsilon^{\frac{2}{3}}\sigma/\Delta h^{\infty}$ is obtained when $n \to \infty$. $\Delta\varsigma$ is the rate of change of the melting enthalpy with system size. It can be expressed in terms of the solid and liquid surface tensions, and the entropy variation during the phase change. This relation is achieved from the Helmholtz free energies [11]:

$$A_{x(T_{\mathrm{m}})} n = A^{\infty}_{x(T_{\mathrm{m}})} n + F\sigma_x \tag{19}$$

noting that the total energies present in equations (15) and (16) are molar values and that at zero pressure,

$$A^{\infty}_{\mathrm{l}(T_{\mathrm{m}})} = A^{\infty}_{\mathrm{s}(T_{\mathrm{m}})}. \tag{20}$$

Equation (19) for solid and liquid takes, respectively, the forms:

$$A_{\mathrm{s}(T_{\mathrm{m}})} = A^{\infty}_{\mathrm{s}(T_{\mathrm{m}})} + 6\sigma_{\mathrm{s}}\upsilon_{\mathrm{s}}^{\frac{2}{3}} n^{-\frac{1}{3}} \tag{21}$$

$$A_{\mathrm{l}(T_{\mathrm{m}})} = A^{\infty}_{\mathrm{l}(T_{\mathrm{m}})} + 3^{\frac{2}{3}}(4\pi)^{\frac{1}{3}}\sigma_{\mathrm{l}}\upsilon_{\mathrm{l}}^{\frac{2}{3}} n^{-\frac{1}{3}}. \tag{22}$$

The resulting change from solid to liquid is then

$$\Delta A = \left(3^{\frac{2}{3}}(4\pi)^{\frac{1}{3}}\sigma_{\mathrm{l}}\upsilon_{\mathrm{l}}^{\frac{2}{3}} - 6\sigma_{\mathrm{s}}\upsilon_{\mathrm{s}}^{\frac{2}{3}}\right) n^{-\frac{1}{3}} \tag{23}$$

that is

$$\Delta h = T_{\mathrm{m}}\Delta S + \left(3^{\frac{2}{3}}(4\pi)^{\frac{1}{3}}\sigma_{\mathrm{l}}\upsilon_{\mathrm{l}}^{\frac{2}{3}} - 6\sigma_{\mathrm{s}}\upsilon_{\mathrm{s}}^{\frac{2}{3}}\right) n^{-\frac{1}{3}}. \tag{24}$$

Since entropy should approximately change as $\Delta S = \Delta S^{\infty} + \Delta\vartheta n^{-1/3}$, where $\Delta\vartheta$ is the difference between the entropy rate of change, in the solid and liquid, with system size, and $\Delta h^{\infty} = T_{\mathrm{m}}\Delta S^{\infty}$, it finally becomes

$$\Delta h = \Delta h^{\infty} + \left(T_{\mathrm{m}}\Delta\vartheta + 3^{\frac{2}{3}}(4\pi)^{\frac{1}{3}}\sigma_{\mathrm{l}}\upsilon_{\mathrm{l}}^{\frac{2}{3}} - 6\sigma_{\mathrm{s}}\upsilon_{\mathrm{s}}^{\frac{2}{3}}\right) n^{-\frac{1}{3}}. \tag{25}$$

It should be noted that, with this level of approximation to Δh, equation (14) predicts the evolution of the melting point as a function of the cluster size with a close profile to the one of Sambles's model [1]. Nonetheless, as previously noted by Chushak [1], about the models proposed by Pawlow, Sambles and himself, equation (14) is not always applicable, since it relies on the assumption that k is independent of nucleus wetting level, even at the limit conditions of no wetting. Consequently, it is not, in general, expectable that equation (14) may correctly predict the melting point of a finite system. In the context of the development of the present model, it is relevant, however, to check out this approximation against simulation or experimental results. In fact, simulations to be reported [12,13], show that for LiCl and NaI clusters the approximation is surprisingly good.

3 Application of the model to KCl clusters

Simulation results [10,13,14] show that early melting is present for LiCl and NaI, but not for KCl clusters. Thus, the present model is expected to be applicable to KCl clusters only in the energy domain $\left]E_{\mathrm{s}(T_{\mathrm{m}})}, E(T_{\mathrm{inf}})\right[$.

Table 1. Energies (kJ mol^{-1}) of the solid and liquid at the bulk melting point (1049 K) for KCl clusters of different sizes (n).

n	$E_{s(T_m)}$	$E_{l(T_m)}$
5832	−642.3	−617.3
4096	−641.1	−616.6
2744	−639.7	−615.8
1728	−638.0	−614.6
1000	−636.1	−613.0
512	−632.1	−611.1

In order to apply the model to a particular material, values for the thermodynamical parameters in equations (4) and (6) are needed. The energies $E_{s(T_m)}$ and $E_{l(T_m)}$ for KCl clusters, used in equation (4), have been obtained from simulation results and are listed in Table 1. Equation (17) was used with $\Delta h^\infty = 26.5$ kJ mol^{-1} and $\Delta\varsigma = 34.4$ kJ mol^{-1}. The average of the bulk solid and liquid heat capacities near the melting temperature, $C_p = 70$ J K^{-1} mol^{-1}, was taken accordingly to the assumption referred to before. Despite all the parameters necessary to compute k are available, we have chosen to estimate k^∞ (note that both are related through Eq. (18)) from the simulation data. $k^\infty = 0.769$ was obtained, by trial and error, in order to make the predicted values correspondent to the domain $]E_{s(T_m)}, E(T_{inf})[$ as close as possible to the simulated ones. The consistency of this value was tested by computing the surface tension presented in Section 4.

Figure 2 displays the phase diagrams for KCl clusters reported in our recent article [10] but, now, including the model predictions. The more noticeable divergences are, as expectable, for the 512 and 1000 ions clusters, but even for those cases the predictions are not incongruent, if the early melting region is excluded.

Equation (14), and also the models discussed by Chushak [1], are not applicable to potassium chloride clusters since early melting is not, in general, observed. In fact, the melting points for cluster sizes over 216 ions are near to the bulk value.

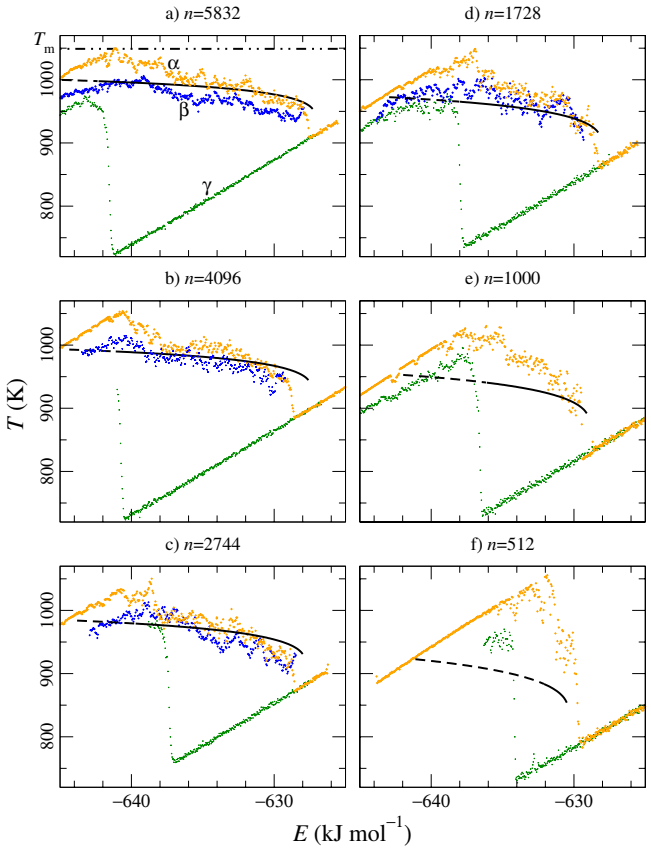

Fig. 2. (Color online) Predictions of the solid-liquid coexistence for KCl clusters (full line); (dashed) early melting region. Simulation results: heating is in orange (α), nucleated cooling is in blue (β), non nucleated cooling is in green (γ).

4 Properties

4.1 Interfacial surface tension

We have reported elsewhere [10], the value $\sigma = 154$ mJ m^{-2} for the interfacial surface tension on the solid-liquid interface, estimated from equation (7):

$$\sigma = \frac{1}{4} k \Delta h v^{-\frac{2}{3}}. \tag{26}$$

As the present model accounts for the thermal balance between droplet and seed, expressed by equation (4), an improved result is expected.

The value $\rho = 1/v = 28.65$ nm^{-3} was obtained for the 512 ions solid system, under periodic boundary conditions at zero pressure and a temperature near T_m. The resulting value is $\sigma = 1/4 \times 0.769 \times 26.5 \times 28.65^{2/3}$ kJ mol^{-1}nm^{-2} $= 79.2$ mJ m^{-2}, in the same order of magnitude of Fiechter's [15] $\sigma_s = 168$ mJ m^{-2} and Sato's [16] $\sigma_l = 97.83$ mJ m^{-2} experimental results. Moreover, from Antonov's rule [1] $\sigma = \sigma_s - \sigma_l = 70.2$ mJ m^{-2} was expected. Despite the actual prediction is much better than the one previously reported, this result should not be overemphasised since the model does not take into account partially unwetted nuclei.

4.2 Molar fractions

A direct sub-product of the model is the liquid molar fraction:

$$\chi_{liq} = \frac{n - \left(\frac{kT_m}{T_m - T}\right)^3}{n}. \tag{27}$$

Figure 3 shows the simulation results [10], obtained with a method based in the analysis of the velocity autocorrelation functions described elsewhere [14], compared with the model predictions for potassium chloride clusters with 2744, 4096 and 5832 ions.

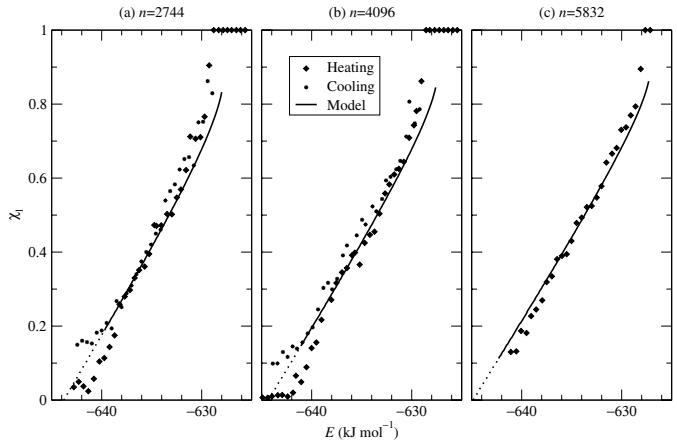

Fig. 3. Prediction of the liquid molar fraction as a function of energy for KCl clusters of different sizes. Simulation results from heating and cooling.

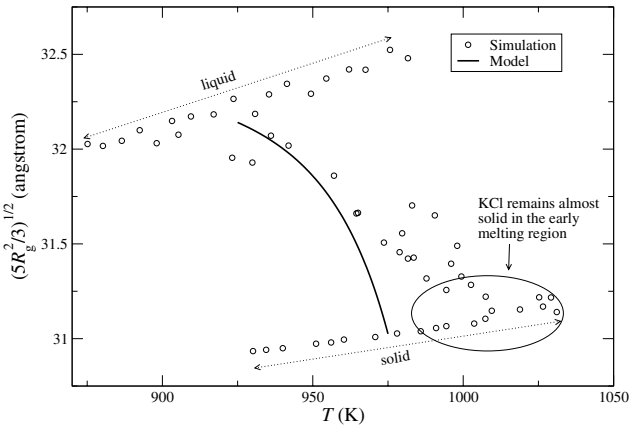

Fig. 4. Prediction of the radius of gyration as a function of temperature for a KCl cluster with 2744 ions.

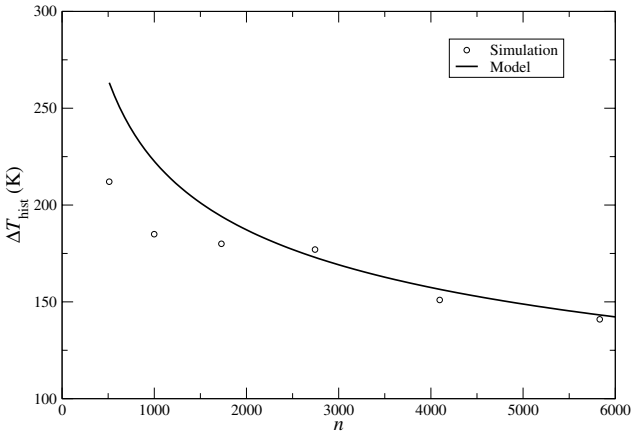

Fig. 5. Prediction of the hysteresis degree as a function of system size for KCl clusters.

4.3 Volume and radius of gyration

The volume, V_C, of the cluster can be estimated from

$$V_C = n\upsilon_l + \left(\frac{kT_m}{T_m - T}\right)^3 (\upsilon_s - \upsilon_l) \tag{28}$$

where υ_s and υ_l are, respectively, the solid and liquid specific volumes. Since density does not sharply vanishes at the cluster surface [11], in unconstrained conditions, this prediction must be corrected by a term proportional to $V_C^{2/3}$ in order to obtain the effective volume.

Assuming an approximate spherical symmetry for the cluster in the phase coexistence region, the radius of gyration,

$$R_g^2 = \frac{3}{5}R^2 \tag{29}$$

becomes

$$R_g^2 = \frac{3}{5}\left\{\left[\frac{3}{4\pi}\left(n\upsilon_l + \left(\frac{kT_m}{T_m - T}\right)^3 (\upsilon_s - \upsilon_l)\right)\right]^{\frac{1}{3}} + c\right\}^2 \tag{30}$$

where c is the additional contribution due to the diffuse surface.

Figure 4 presents the prediction for 2744 ions compared with the simulation results; the value of $c = 1.8$ Å was used.

4.4 Hysteresis

The intrinsic degree of hysteresis may be defined from equation (10) as

$$\Delta T_{hist} = T_m - T_{inf} = \left(\frac{3k^3\, {T_m}^3\, \Delta h}{nC_p}\right)^{\frac{1}{4}} \tag{31}$$

or more rigorously

$$\Delta T_{hist} = T_m - T_l(E(T_{inf})) \tag{32}$$

where $E(T_{inf})$ is the energy of the cluster at temperature T_{inf} given by equation (11). After some algebra,

$$T_l(E(T_{inf})) = T_m - \left(3^{\frac{1}{4}} + 3^{-\frac{3}{4}}\right)\Delta h^{\frac{1}{4}}\,(kT_m)^{\frac{3}{4}}\,(C_p n)^{-\frac{1}{4}} \tag{33}$$

and finally

$$\Delta T_{hist} = \left(3^{\frac{1}{4}} + 3^{-\frac{3}{4}}\right)\Delta h^{\frac{1}{4}}\,(kT_m)^{\frac{3}{4}}\,(C_p n)^{-\frac{1}{4}}\,. \tag{34}$$

For systems that present early melting

$$\Delta T_{hist} = T_{if} - T_l(E(T_{inf})) \tag{35}$$

$$= -T_m k n^{-\frac{1}{3}} + (3^{\frac{1}{4}} + 3^{-\frac{3}{4}})\Delta h^{\frac{1}{4}}(kT_m)^{\frac{3}{4}}(C_p n)^{-\frac{1}{4}}. \tag{36}$$

These results show some properties of the clusters approaching the bulk as a function of $n^{-1/4}$ instead of $n^{-1/3}$.

Figure 5 display the comparison between model prediction and values inferred from simulations. The intrinsic degree of hysteresis approaches zero as $n \to \infty$.

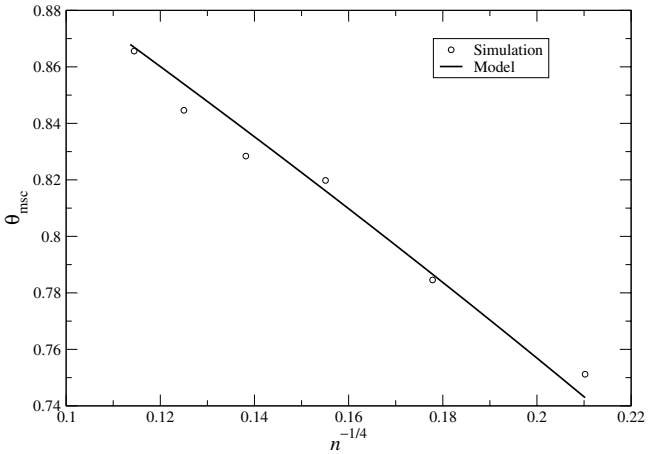

Fig. 6. Prediction of the minimum extent of supercooling as a function of system size for KCl clusters.

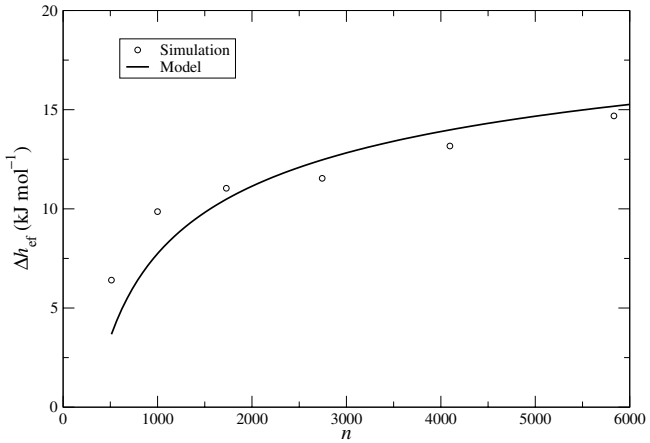

Fig. 7. Prediction of the effective enthalpy of melting as a function of system size for KCl clusters.

4.5 Minimum extent of supercooling

The temperature given by equation (33) is the highest temperature where the system can start a liquid to solid transition. It defines the minimum extent of supercooling

$$\theta_{\rm msc} = T_{\rm l}(E(T_{\rm inf}))/T_{\rm m} \tag{37}$$

that a droplet should attain during the freezing process before it can crystallise. Figure 6 shows the comparison between the model predictions and the simulation results.

4.6 Effective enthalpy of melting

The difference

$$\begin{aligned}\Delta h_{\rm ef} &= E(T_{\rm inf}) - E_{\rm s(}T_{\rm m)} &(38)\\ &= \Delta h - \left(3^{\frac{1}{4}} + 3^{-\frac{3}{4}}\right)\Delta h^{\frac{1}{4}}\left(kT_{\rm m}C_p\right)^{\frac{3}{4}} n^{-\frac{1}{4}} &(39)\end{aligned}$$

gives the effective enthalpy of melting in a system without early melting. In a calorimeter with a fixed energy flux, it corresponds to the energy slowly transferred to the system, starting from the point where the temperature ceases to increase, up to the point where it starts to increase again (see Fig. 2).

In case of early melting it will be instead

$$\begin{aligned}\Delta h_{\rm ef} &= E(T_{\rm inf}) - E_{\rm if} &(40)\\ &= \Delta h + kC_pT_{\rm m}n^{-\frac{1}{3}}\\ &\quad - (3^{\frac{1}{4}} + 3^{-\frac{3}{4}})\Delta h^{\frac{1}{4}}(kT_{\rm m}C_p)^{\frac{3}{4}}n^{-\frac{1}{4}}. &(41)\end{aligned}$$

Figure 7 shows the comparison between the model prediction and simulation results.

4.7 Heat capacity

Assuming early melting, the heat capacity along the phase coexistence region , c_p, can be obtained from equation (9):

$$c_p = \left(\frac{\partial E}{\partial T}\right)_p = C_p - 3k^3\frac{\Delta h\ {T_{\rm m}}^3}{n(T_{\rm m}-T)^4}. \tag{42}$$

The minimum, negative, value for c_p will occur at the beginning of the early melting, that is substituting (14) in (42),

$$c_p|_{T=T_{\rm if}} = C_p - 3\frac{\Delta h}{T_{\rm m}k}n^{\frac{1}{3}}. \tag{43}$$

This approaches infinity, by negative values, when $n \to \infty$.

The maximum value is attained at the end of the melting, that is substituting (10) in (42),

$$c_p|_{T=T_{\rm inf}} = C_p - C_p = 0. \tag{44}$$

As the system dimension becomes close to infinity, the interval where c_p is finite narrows to this single point since $T_{\rm inf}$ approaches $T_{\rm m}$.

The global heat capacity on melting ζ_p, that is the quotient of the energy that is needed to melt the system by the temperature change during the process, is

$$\begin{aligned}\zeta_p &= \frac{\Delta h_{\rm ef}}{T_{\rm l}(E(T_{\rm inf})) - T_{\rm if}} &(45)\\ &= \frac{\Delta h + kC_pT_{\rm m}n^{-\frac{1}{3}} - (3^{\frac{1}{4}} + 3^{-\frac{3}{4}})\Delta h^{\frac{1}{4}}(kT_{\rm m}C_p)^{\frac{3}{4}}n^{-\frac{1}{4}}}{T_{\rm m}kn^{-\frac{1}{3}} - (3^{\frac{1}{4}} + 3^{-\frac{3}{4}})\Delta h^{\frac{1}{4}}(kT_{\rm m})^{\frac{3}{4}}(C_pn)^{-\frac{1}{4}}} &(46)\end{aligned}$$

and approaches infinity, by negative values, when $n \to \infty$.

In the absence of early melting it becomes instead:

$$\begin{aligned}\zeta_p &= \frac{\Delta h_{\rm ef}}{T_{\rm l}(E(T_{\rm inf})) - T_{\rm m}} &(47)\\ &= -\frac{\Delta h - \left(3^{\frac{1}{4}} + 3^{-\frac{3}{4}}\right)\Delta h^{\frac{1}{4}}\left(kT_{\rm m}C_p\right)^{\frac{3}{4}}n^{-\frac{1}{4}}}{\left(3^{\frac{1}{4}} + 3^{-\frac{3}{4}}\right)\Delta h^{\frac{1}{4}}\left(kT_{\rm m}\right)^{\frac{3}{4}}\left(C_pn\right)^{-\frac{1}{4}}} &(48)\end{aligned}$$

with the same asymptotic behaviour as (45).

As the heat capacity is a derivative and the simulation results have considerable fluctuations in the coexistence region, the comparison of the model predictions with simulations will be presented in a future report.

5 Concluding remarks

A model to predict the solid-liquid coexistence of unconstrained clusters and to correlate their properties has been proposed. The model predictions compare well with simulation results, suggesting that critical conditions of the solid nuclei are prevalent over other contributions. All the derived equations yield the right bulk limit when the number of particles approaches the thermodynamic limit.

The application of the model to the prediction and interpretation of different solid phases in lithium chloride and to the phase behaviour of other alkali halide clusters is in progress and will be reported soon [12,13].

The improvement of the model in order to predict the existence or absence of early melting is one of the perspectives to future work. Moreover, the need to deal with the vapour pressure of more volatile substances also claims for an extension of the model.

Despite alkali halide aggregates can be observed in the absence of applied external pressure for considerable lifetimes, significant values are expected for the internal pressure in small clusters due to the large fraction of surface particles and small surface curvature radius. These values should approach the bulk one (which is the reference state of the present model) as the cluster sizes approach infinity. In this limit, they are virtually zero for unconstrained systems and nearly zero for solid and liquid alkali halides in equilibrium with their vapour pressures up to the boiling point. Indeed, it is well known from experiment that ionic salts present, even in the liquid state, very low vapour pressures. The derivation of the internal pressure from the model, and its comparison with simulation results, is also in perspective to further development.

One of us (P. Rodrigues) gratefully acknowledges the institutional support of the Department of Chemistry and Biochemistry, FCUL, during his research work. We thank Intel Corporation for the free access to their compilers and the GNU and Linux communities for all the invaluable tools they offer.

References

1. Y.G. Chushak, L.S. Bartell, J. Phys. Chem. B **105**, 11605 (2001)
2. G. Wulff, Z. Kristallogr. **34**, 449 (1901)
3. I.V. Markov, *Crystal grouth for beginners*, 3rd edn. (World Scientific Publishing Co. Pte. Ltd., 1998)
4. K. Binder, Physica A **319**, 99 (2003)
5. C.L. Cleveland, U. Landman, W.D. Luedtke, J. Phys. Chem. **98**, 6272 (1994)
6. C. Rottman, M. Wortis, Phys. Rev. Lett. **52**, 1009 (1984)
7. C. Rottman, M. Wortis, Phys. Rev. B **29**, 328 (1984)
8. C. Rottman, M. Wortis, Phys. Rep. **103**, 59 (1984)
9. P.C.R. Rodrigues, Ph.D. thesis, Faculdade de Ciências, Universidade de Lisboa (2006)
10. P.C.R. Rodrigues, F.M.S. Silva Fernandes, Eur. Phys. J. D **40**, 115 (2006)
11. P.G. Debenedetti, *Metastable Liquids, Concepts and Principles* (Princeton University Press, New Jersey, 1996)
12. P.C.R. Rodrigues, F.M.S. Silva Fernandes, Eur. Phys. J. D (to be submitted)
13. P.C.R. Rodrigues, F.M.S. Silva Fernandes, Eur. Phys. J. D (to be submitted)
14. P.C.R. Rodrigues, F.M.S. Silva Fernandes, Int. J. Quant. Chem. **84**, 169 (2001)
15. S. Fiechter, Sol. Energy Mater. Sol. Cells **83**, 459 (2004)
16. Y. Sato, T. Ejima, M. Fukasawa, K. Abe, J. Phys. Chem. **94**, 1991 (1990)